IEEE Access
Multidisciplinary | Rapid Review | Open Access Journal

Received July 25, 2019, accepted August 5, 2019, date of publication August 8, 2019, date of current version August 22, 2019.

Digital Object Identifier 10.1109/ACCESS.2019.2933881

Fault Monitoring and Diagnosis of Actuators in Electromagnetic Valve-Train Based on Neural Networks Optimization Algorithm

TONGJUN GUO[1], SIQIN CHANG[1], ZHIQIANG CHEN[1], HANGANG HUANG[2], AND JIANGTAO XU[3]

[1]School of Mechanical Engineering, Nanjing University of Science and Technology, Nanjing 210094, China
[2]College of Technology and Art Jingdezhen Ceramic Institute, Jingdezhen 333001, China
[3]School of Mechanical Engineering, Nanjing Institute of Technology, Nanjing 211167, China

Corresponding author: Tongjun Guo (gtj0731@163.com)

This work was supported by the National Natural Science Foundation of China under Grant 51306090.

ABSTRACT In order to realize fully flexible variable valve lift and improve the intake efficiency of the engine, a new electromagnetic valve-train (EMVT) was designed to replace the traditional CAM in the engine valve-train. However, as the durability of electromagnetic linear actuator (ELA) in the EMVT was lower than that of CAM, and there might be some problems during a long running time. This paper presented an improved online fault diagnosis method combining BP Neural Networks with Grey Relation Analysis (GRA) to analyze current signals, which could realize the monitoring, diagnosis of electromagnetic linear actuator faults and early warning so as to prevent unnecessary situations such as accidental cylinder stop of the engine. The results showed that this method had a high fault diagnosis rate, high speed, reliability and practicability.

INDEX TERMS BP neural networks, electromagnetic linear actuator, fault diagnosis, grey relation analysis, status monitoring.

I. INTRODUCTION

The development of engine valve-train has gone through three stages: conventional CAM drive valve-train, variable CAM drive valve-train and camless drive valve-train. In the conventional CAM drive engine, the valve movement was driven by the CAM mechanism, and the valve movement is fixed relative to the crankshaft Angle. In the variable CAM drive engine, the valve timing or lift was changed by Variable Valve Timing technology, but the adjustment was still limited by CAM profile, and could only meet part of the working conditions. In the camless drive valve-train, each valve could be driven by a separate actuator, which completely got rid of the constraint of CAM profile, and realized flexible adjustment of valve timing, valve opening duration and valve lift [1].

There are three types of camless drive valve-train: hydraulic, electro-mechanic, electromagnetic type [2], [3]. The performance of hydraulic actuator for the camless technology depends on the external temperature with the oil viscosity. It is based on the application of oil under pressure and piezo-valve acting on the valve of engine valve. The electro-mechanical actuators use a mechanical system using springs and a brushless motor to act the valves, which is difficult to integrate into vehicles due to lack of compactness. The electromagnetic actuators convert electrical energy into mechanical energy by electromagnetic induction principle. It can realize fully flexible adjustment of valve timing, valve lift and valve opening duration according to engine working conditions, so as to realize the optimal performance of the engine in each working condition and improve engine performance [4]–[6]. Electromagnetic linear actuator (ELA) is one of the electromagnetic actuators, which also known as ''linear motor''. Unlike the traditional rotary motor, it can directly convert electrical energy into mechanical energy of linear motion, without any intermediate conversion device. Besides, the electromagnetic linear actuator has advantages of simple structure, fast response and high precision motion performance. At home and abroad, new high-performance electromagnetic linear actuators are still under development [7], [8]. Our research group conducted an in-depth research on the self-developed ELA, mainly optimized and improved the structure, control algorithm of the actuator, and successfully

The associate editor coordinating the review of this manuscript and approving it for publication was Yongping Pan.

applied it into the engine valve mechanism to replace the traditional CAM device [9]–[11].

Since the camless electromagnetic drive valve-train was a nonlinear system, its main difficulties lay in the motion control accuracy and nonlinear compensation of electromagnetic linear actuator. At present, researchers at home and abroad are conducting in-depth research on it. Mercorelli [12] designed a new type of electromagnetic linear motor driven valve-train and proposed a sensorless control strategy based on input current and voltage measurement to control the actuator displacement, which was beneficial to reduce the system structure. Dimitrova *et al*. [3] introduced the innovative application of electromagnetic actuator in variable engine valve-train. It proposed a control strategy both with nonlinear feedforward actions and with a linear robust feedback controller, which was able to reject all what cannot be predicted and improved the robustness of the system and had better dynamic performance.

In addition, the durability of electromagnetic linear actuator in the electromagnetic driven valve-train was particularly worthy of attention, and was often overlooked. This was because the research of electromagnetic linear actuator was usually carried out durability test under experimental conditions, however, there was still a gap with the real engine environment. Due to the complicated environment inside the engine cylinder, the electromagnetic linear actuator inevitably broke down after a long running time. Therefore, it was particularly important to monitor the operating state of the actuator, predict the fault ahead, diagnose the fault and locate it, and we could reduce unnecessary losses caused by the engine failure when the actuator had faults.

In the past, the method of monitoring faults in electrical equipment relied heavily on the workers experience to judge the health of the equipment based on the acoustic and thermal aspects of the DC motor [13], [14]. In addition, the maintenance of the motor equipment was planned and managed no matter the motor equipment was faulty or not. Recently, there were many scholars researching on the monitoring system of motor, the main research contents were industrial equipment operation status monitoring, fault diagnosis and early warning. Its purpose was to reduce production costs, increase efficiency and productivity, and achieve intelligent industrial control, safety and emergency [15], [16].

In recent years, with the development of computer information technology, artificial intelligence methods and signal processing technologies, more and more advanced algorithms have been applied to the online fault diagnosis of DC motors. There were many papers at home and abroad that had presented a variety of motor fault diagnosis methods mainly were classified into three categories:

(1) Mathematical algorithms and models: The articles often used advanced algorithms to establish diagnostic models, such as fuzzy reasoning, artificial neural networks, Bayesian reasoning, Dempster-Shafer evidence theory, support vector machines, wavelet analysis, genetic algorithms, etc [17]–[22].

(2) Fault diagnosis basis: The articles often chose armature voltage, armature current, speed, torque, motor temperature of DC motor as the fault diagnosis basis [23]–[26].

(3) Signal processing methods: The papers often used methods, such as Fourier transform, wavelet transform, parameter identification, etc. to process the acquired signals [27]–[30].

The analysis and processing of the motor fault signal is the key to solve the fault diagnosis problem. The core of the method is to analyze the characteristics of parameter variation of the motor. The research objects of the above references were all rotating electric machines, and there was no research literature on ELA and linear motor yet.

The contribution of this paper was the innovative use of the self-developed electromagnetic linear actuator in engine valve-train. The actuator was characterized by performant and efficient magnetic circuit, direct driven by the current, fast response time, lightweight moving parts, arbitrarily variable motion displacement, high control accuracy robustness, which were conducive to improving engine efficiency, reducing fuel consumption and reducing carbon dioxide emissions. At the same time, this paper adopted the improved artificial neural network method to monitor the motion state and predict fault in advance of electromagnetic linear actuator, and made the recognition rate and training speed of the optimized system greatly improved. This method was conducive to real-time online monitoring and improving the defects of previous fault diagnosis work. In addition, this method only needed to analyze the current signal acquisition of actuators, do not needed other sensor signals, which was benefit of simplifying the system structure, reducing cost, improving reliability and had a high practicability and application prospect. It could provide powerful guarantee for the application of electromagnetic drive valve-train, routine maintenance and detection of the vehicles.

This article expanded from the following aspects:

(1) Analyzed faults of electromagnetic linear actuator.

(2) Proposed an improved algorithm of BP neural network based on grey correlation optimization, and established a systematic training model for fault monitoring and diagnosis of electromagnetic linear actuator

(3) Performed test experiments and compared it with the pre-optimization diagnosis method.

II. FAILURE ANALYSIS OF ELECTROMAGNETIC LINEAR ACTUATOR IN ELECTROMAGNETIC VALVE-TRAIN

A. DESIGN OF ELECTROMAGNETIC LINEAR ACTUATOR

1) THE PRINCIPLE, DESIGN AND PARAMETERS OF ELECTROMAGNETIC LINEAR ACTUATOR

The self-developed dynamic coil electromagnetic linear actuator was adopted in the electromagnetic valve-train, as shown in Fig.1. The actuator was mainly composed of internal magnetic choke, external magnetic choke, permanent magnet, electromagnetic coil and skeleton. Since the electromagnetic coil is subject to the axial electromagnetic force in the air

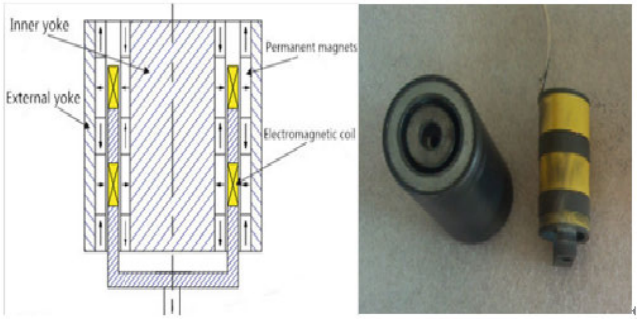

FIGURE 1. Self-developed electromagnetic linear actuator structure.

gap magnetic field, the specific motion law of the valve can be realized by controlling the magnitude and direction of the driving current [8], [9].

In the electromagnetic linear actuator, the magnetic flux must looped through the inner and external yokes. Therefore, the inner and external yokes of actuator should be made of higher magnetic permeability, less coercive force and saturation magnetization material. We chose 08 steel after comparison.

In the electromagnetic linear actuator, the permanent magnet adopted a high-performance permanent magnet material-NdFeB, which had high residual magnetic flux density and coercive force. The permanent magnets were arranged in an array of eight magnetic tile splicing schemes. It was benefit of enhancing the magnetic flux density in the air gap and reducing the saturation of the yoke [31].

In the electromagnetic linear actuator, the coil was wound on the specific shape framework with equal length opposite direction and cascade. The coil framework was made of epoxy resin material with high mechanical strength, non-conductivity, good machinability and low density, which was benefit of reducing the mass of the mover. The coil adopted Polyimide enameled round copper wire with a line temperature index of 220 (QY-2/2000.100GB6109.6-1988).

Recently, the driving voltage was increased from the original 24v to 42v to meet the requirements for improving the system response speed and overcoming the cylinder pressure for the application in the electromagnetic drive valve-train. The electromagnetic linear actuator has been optimized again. The structure size and parameters of design were shown in Table 1:

TABLE 1. Size and parameters of electromagnetic linear actuator.

Parameter	Quantity	Value
r	Radius	18 mm
h	Height	78 mm
V	Volume	79.4 cm^3
m	Moving mass	94.6 g
R	Resistance	1.3 Ω
L	Inductance	0.94 mH
S	Displacement	8 mm
F_m	Maximum electromagnetic force	360 N
a_m	Maximum acceleration	3806 m/s^2
I_m	Maximum current	30.4 A
U	Driving voltage	42 V
K_e	Back electromotive force constant	12 V • s/m
K_m	Force constant	12 N/A
c	Damping coefficient	2 N/(m • s-1)

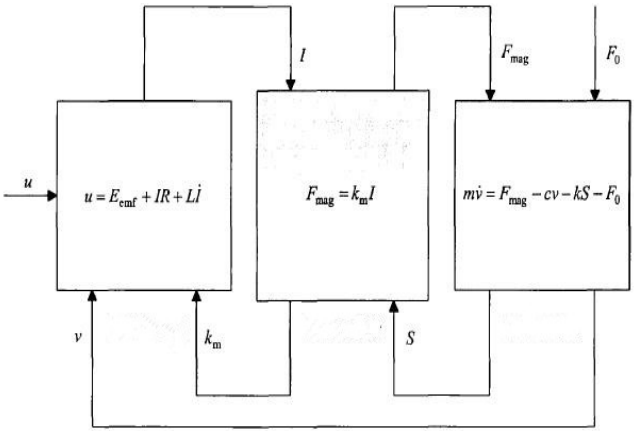

FIGURE 2. Subsystem coupling relationship in ELA.

2) MATHEMATICAL MODEL OF ELECTROMAGNETIC LINEAR ACTUATOR

ELA is a complex systems of machinery, circuit and magnetic circuit coupling each other. As shown in Fig. 2.

The differential equations for ELA are:

$$\begin{cases} \dot{I} = -\dfrac{R}{L}I - \dfrac{k_e}{L}v + \dfrac{u}{L} \\ \dot{v} = \dfrac{k_m}{m}I - \dfrac{c}{m}v - \dfrac{F_0}{m} \\ \dot{S} = v \end{cases} \tag{1}$$

In the formula: m – the quality of motion of electromagnetic linear actuators, including the quality of the skeleton, solenoid and connectors;

v – valve speed, $v = \dot{S}$;

c – damping coefficient;

u – voltage;

I – the current of the coil;

R – coil resistance;

L – coil inductance;

$k_e = BlN$ – back EMF constant;

$k_m = k_b B_\delta lN$ – actuator force constant;

F_0 – External load.

3) IMPACT OF SYSTEM PARAMETER VARIATION

Through the above analysis of the mathematical model of the electromagnetic linear actuator, the simulation model of the whole system was built in Matlab/Simulink, and the key parameters affecting the system performance were discussed.

a: MOVING MASS

The moving mass was one of the important indicator of its dynamic performance. It could be seen from the Fig. 3 that the bigger the moving mass, the slower the system response.

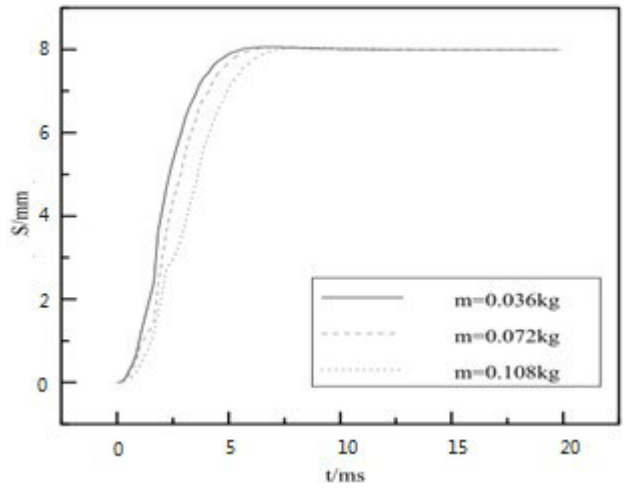

FIGURE 3. The step response of displacement curve under different moving masses.

b: RESISTANCE

When the driving voltage was constant, the variation of the coil resistance directly affected the current change up to affecting the response of system. It could be seen from the Fig. 4 that the larger the coil resistance, the slower rising speed of the coil current, the smaller the peak current and the slower the system response.

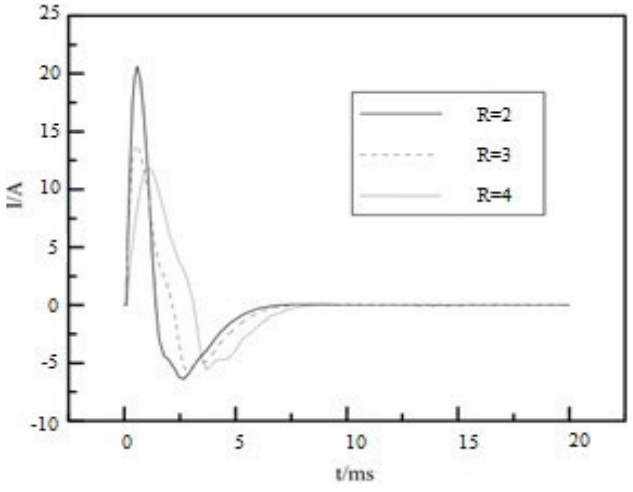

FIGURE 4. The current curve under different resistance.

c: DIFFERENT DRIVING VOLTAGE

The magnitude of the driving voltage directly determined the rising speed of the coil current up to affecting the response of system. It could be seen from the Fig. 5 that the larger driving voltage, the faster rising speed of the coil current, the larger the driving electromagnetic force and the more quick the system response.

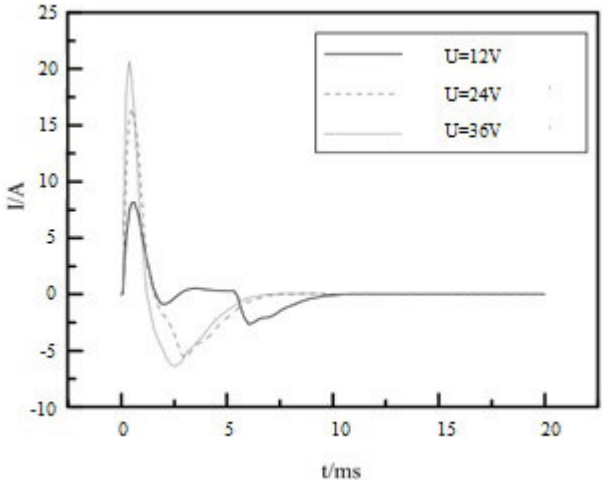

FIGURE 5. The current curve under different driving voltage.

B. FAULT ANALYSIS OF ELECTROMAGNETIC LINEAR ACTUATOR

We first analyzed the possible fault conditions of the ELA.

1) ACTUATOR SHORT CIRCUIT

As can be seen from the Fig.6, after running 300 hours, the surface of the enameled wire between the coil and the outer yoke became black. By optimizing the structure of electromagnetic linear actuator, the air gap width was set to 6mm, the coil framework width was set to 1mm, the coil area width was set to 4.5mm, and 0.25mm gap was left both sides. The coil frame was symmetrically placed between the inner magnetic yoke and permanent magnet. Theoretically, the coil framework was not affected by the radial force in the moving process and not appeared wear. There were two reasons for wear by analyzing, on the one hand, due to small deviation of the actual processing and assembly process; On the other hand, due to the engine cylinder environment complex, and the materials expanded by thermal and overheating. It was

FIGURE 6. The picture of actuator coil's enameled wire abrasion after running 300 hours.

inferred that the coil electrically connected to the outer yoke and external yoke after a long running time, and caused short circuit. The main symptom was the current variation.

2) ACTUATOR DISCONNECTION

As can be seen from the Fig.7, after running 300 hours, it was found that the outer wiring of the coil weared. It was inferred that it might cause poor contact and disconnection at the line joint after a long running time. This type of fault was mainly caused by excessive load, material defects of the body and the like. The main symptom was the significantly current variation.

FIGURE 7. The picture of actuator coil wiring after running 300 hours.

3) SKELETON DEFORMATION

It could be seen from the Fig.8 that after running 300 hours, the surface of the skeleton had worn marks and burrs. It could be inferred that the coil skeleton might be deformed after a long period of operation. The main reason was that in the actuator design, the coil skeleton made of PTFE material was subjected to thermal expansion and uneven force during the movement, resulting in wear and deformation. The main symptoms were the vibration and noise of motor becoming bigger.

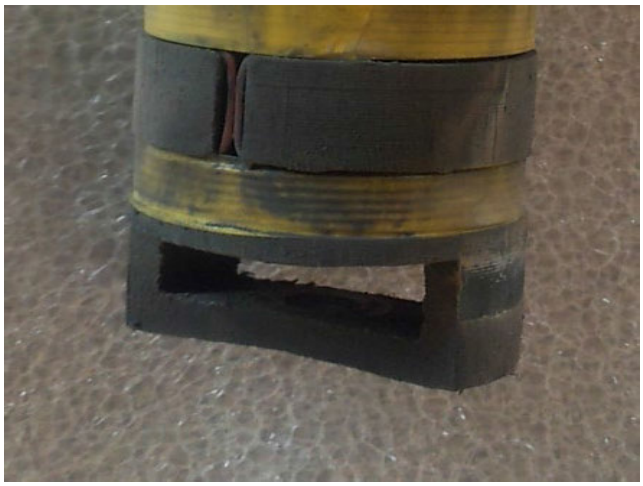

FIGURE 8. The picture of actuator skeleton after running 300 hours.

Through the above analysis, we could find out that when the actuator failed, the parameters of actuator changed, so we could monitor and diagnose faults by the actuator's self-parameters, but the monitoring data was large, and some data was not easy to measure, so we should extract the fault characteristic parameters from the easily measured and less data. The main parameters of the actuator corresponding to the three fault types were shown in Table 2.

TABLE 2. The type of actuator faults and the main corresponding parameters.

Fault type	Main variable parameter of actuator
Actuator short circuit	R_a , L_a
Actuator disconnection	R_a
Skeleton deformation	c, m

C. EXTRACTING THE FAULT CHARACTERISTIC PARAMETERS OF ACTUATOR

According to the dynamic differential equations (1) for solving electromagnetic linear actuators and the above fault analysis, we could find that the change of the parameters of the actuator caused the change of the current signal. In addition, the current signal of the actuator was easily collected. Therefore, we used the actuator current signal as the basis of the analysis, and sought the characteristic parameters of fault diagnosis system, and analyzed the relationship between the characteristic parameters, the actuator parameters and the actuator fault types.

1) THE STARTING CURRENT I_m

When the actuator starts, its current curve was an approximate exponential curve. The maximum value of current I_m is very close to the value at time $t = 0$:

$$i_m \approx i(0) = \frac{U}{R_a} \tag{2}$$

It could be seen from Eq. (2) that the resistance of the actuator directly affected I_m, this was good for determining faults, so this paper put I_m as the first characteristic parameter for on-line monitoring and fault diagnosis of ELA.

2) THE DROP RATE OF STARTING CURRENT K_I

$$K_i = -\frac{i_m}{T_m} = -\frac{U \cdot \mathrm{k_m^2}}{\mathrm{m}R_a^2} \tag{3}$$

The time constant of an electromagnetic linear actuator was an important indicator of its dynamic performance, mainly including the electrical time constant $T_e = L_a/R_a$ and electromechanical time constant $T_m = mR_a/k_m^2$. In general, the electromechanical time constant was always much larger than the electrical time constant. The drop rate of starting current K_i depended on electrical time constant T_m.

The larger T_m, the slower the current drops. The expression also showed that the change of electromechanical time constant could be affected by the mass of the mover m and the resistance of the coil R_a.When some fault occurred, the above three parameters would inevitably be changed, and these changes would eventually reflected on the drop rate of starting current. Therefore, this paper put the drop rate of starting current K_i as the second characteristic parameter of on-line monitoring and fault diagnosis of ELA.

3) THE STEADY-STATE CURRENT I_a

The equations for steady-state operation of electromagnetic linear actuator was as follows:

$$\begin{cases} U = R_a i + k_e v \\ k_m i = cv + F_0 \end{cases} \tag{4}$$

The current under steady-state operation of the actuator was obtained by solving the above equations:

$$I_a = \frac{cU + k_e F_0}{k_m k_e + cR_a} \tag{5}$$

According to Eq. (5), steady-state current I_a mainly depended on the external load F_0, as well as the value of the resistance of the actuator R_a, friction coefficient c. Therefore, the paper put the steady-state current I_a as the third characteristic parameter of online fault diagnosis of actuator.

Through the above analysis, all of the above three characteristic parameters were closely related to the actuator current. According to Eq. (2), (3) and (5), the intrinsic relationship between the main parameters of the actuator and the three characteristic parameters could be obtained, as shown in Table 3.

TABLE 3. Characteristic parameters corresponding to the main parameters of actuator.

Parameter of the ELA	The characteristic parameter
R_a	I_m , K_i , I_a
L_a	K_i
c	I_a
m	K_i
F_0	I_a

When the ELA had different faults, the type, direction (large or small) and variation amplitude of the characteristic parameters were different. By comparing the characteristic parameters of the faulty state with the normal state, we could comprehensively determine whether the actuator was faulty and which type of fault it was.

In addition, in the Eq. (1), external disturbances such as voltage changes and load changes might also cause changes in the characteristic parameters. Therefore, separate analysis was needed to distinguish them. Particularly, the load disturbance was random, difficult to predict and monitor, so this paper considered the load disturbance as a special type of fault.

III. SOFTWARE AND HARDWARE DESIGN OF THE SYSTEM

A. HARDWARE DESIGN FOR THE LOWER COMPUTER

The lower computer hardware consisted of three parts: data acquisition unit and data processing unit, including power module, sensor and synchronous sampling circuit, microprocessor DSP2812 module, etc. Its main function is to collect and preprocess data such as current, voltage and displacement of ELA.

The magnetic balance Hall current sensor TBC200LTHA was used in this system. In order to improve the load capacity of the circuit and filter out high frequency interference, a voltage follower and a second order low pass filter circuit were added at the output of the Hall current sensor.

B. SOFTWARE DESIGN FOR THE SYSTEM

The upper computer software is jointly developed by C# and Matlab. The main function is to carry out online real-time monitoring, analysis and data storage of the operating state of ELA. The software interface includes the number of each actuator, the valve position of the corresponding valve-train, the running status monitoring, the training model of BP neural network, the fault diagnosis and the SQL data storage. If a fault occurs, the faulty actuator immediately displays and an early warning signal is issued, as shown in Fig. 9.

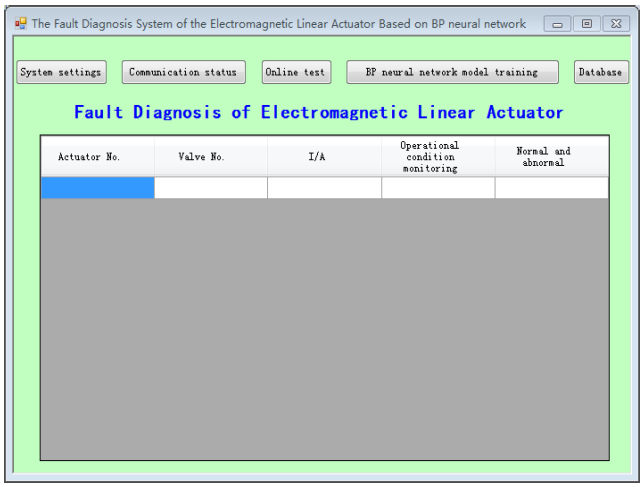

FIGURE 9. Software design.

Among them, the extraction of characteristic parameter and the neural network fault model of electromagnetic linear actuator are mainly realized by calling Matlab software with C#.

IV. THE FAULT DIAGNOSIS SYSTEM OF ELA BASED ON IMPROVED BP NEURAL NETWORK

Since simple structure and strong plasticity, BP neural network is widely used in the fields of function fitting, parameter identification and classification. The fault monitoring and diagnosis of ELA is a classic parameter identification and

classification problem. Therefore, the BP neural network is chosen as the model basis for fault diagnosis in this paper.

The core idea of the BP neural network algorithm is to transform the input and output problems of a set of samples into a nonlinear optimal solution problem. Using the gradient descent method to solve the weights of each layer, the errors are gradually minimized. In the model of the BP neural network, the number of neurons in the input layer and the output layer of the neural network is determined, and the number of neurons which determines the classification ability of the network in the hidden layer is uncertain. Therefore, the correct selection of the number of neurons in the hidden layer is crucial for improving the network recognition performance.

In the current research on the neural network, almost all the neurons in the hidden layer were determined according to the experimental and the empirical formula. Therefore, in order to realize real-time optimization of BP neural network structure and improve the learning speed of model training, this paper proposed Gray Relational Analysis method based on the pre-learning of BP neural network to dynamically adjust the number of neurons in the hidden layer [32]–[38].

A. GRAY RELATIONAL ANALYSIS (GRA)

Based on the mathematical statistics method, the GRA method finds the data (the amount of mapping) that reflects the behavior characteristics and predicts the development trend of the system through the GRA of the behavioral feature data and related factor data. The GRA method is especially suitable for small and irregular samples, which is very consistent with the characteristics of actuator fault diagnosis. The core idea of the GRA method is to judge the relationship of the sequence according to the similarity of the geometrical shapes between the sequence curves (grey correlation degree). The closer the curves of the two sequences, the larger correlation degree of the corresponding sequence.

B. FAULT DIAGNOSIS AND PREDICTION MODEL OF BP NEURAL NETWORK BASED ON GRA OPTIMIZATION

In this paper, the gray relational degree is used to judge the degree between the output of each hidden layer neuron and the expected output, and the actual number of neurons are calculated to optimize the structure of the BP neural network. The main content is:

(1) Calculating the degree of relation between the output of the k-th hidden layer neuron and the expected output (reference sequence);

(2) Judging the magnitude of the effect of the k-th hidden layer neuron on the output layer;

(3) Determining the size of the effect of the initial q hidden layer neurons on the output layer.

For a given degree of association ε, $\varepsilon \in (0, 1)$, if the output of a neuron in the hidden layer is less than the expected output, we think that the influence of the hidden layer's node on the output of the neural network is too small, and it is deleted to achieve the purpose of optimizing the network structure.

Optimizing the calculation parameters of the BP neural network model based on Gray Relational Analysis is as follows:

Given a training samples, $t = 1, 2, \cdots, N$, the number of neurons in the input layer is n, and the number of neurons in the output layer is m, $j = 1, 2 \cdots, m$. Only the number of neurons in the hidden layer q is the amount to be determined, $k = 1, 2, \cdots, q$.

The expected output of the network is set to $y = (y_1, y_2, \ldots y_m)^T, y \in R$.Sequence $y_i = (y_i(1), y_i(2), \ldots y_i(N))$ is the expected output of the N samples corresponding to the i-th output neuron.

Step 1: First, collect the object data $X_i(t)$, $t = 1, 2, \cdots, N$. Then, according to the actual object, the behavioral characteristic sequence (reference sequence) responding system behavior characteristics and the related factor sequence (comparative sequence) affecting the system behavior are determined

Reference sequence: $X_0 = (X_0(1), X_0(2), \cdots, X_0(n))$;

Comparison sequence: $X_i = (X_i(1), X_i(2), \cdots, X_i(n))$.

Step 2: Taking the expected output of the neural network as the reference sequence:

$$y = \begin{bmatrix} y_1 \\ y_2 \\ \vdots \\ y_m \end{bmatrix} = \begin{bmatrix} y_1(1) & y_1(2) & \cdots & y_1(N) \\ y_2(1) & y_2(2) & \cdots & y_2(N) \\ \vdots & \vdots & \vdots & \vdots \\ y_m(1) & y_m(2) & \cdots & y_m(N) \end{bmatrix} \tag{6}$$

Step 3: Taking the output sequence value of the k-th neuron of the hidden layer as the test sequence:

$$h_k = (h_k(1), h_k(2), \cdots h_k(N)) \tag{7}$$

Step 4: Finding the difference sequence according to Eq. (8) and calculating the maximum and minimum of the difference value:

$$\begin{cases} \Delta_i(t) = |x_0(t) - x_i(t)| \\ \Delta_{\max} = \max\limits_{i=1}^{m} \left\{ \max\limits_{t=1}^{n} \{|x_0(t) - x_i(t)|\} \right\} \\ \Delta_{\min} = \min\limits_{i=1}^{m} \left\{ \min\limits_{t=1}^{n} \{|x_0(t) - x_i(t)|\} \right\} \end{cases} \tag{8}$$

Step 5: Calculating the correlation coefficient $r_{ki}(t)$ between the output of the k-th hidden layer's node (comparison sequence) and the reference sequence according to Eq. (9)

$$r_{ki}(t) = r\left(x_k(t), x_i(t)\right) = \frac{\Delta_{\min}(k, i) + \rho\Delta_{\max}(k, i)}{\Delta_{ki}(t) + \rho\Delta_{\max}(k, i)} \tag{9}$$

In the formula, the resolution coefficient $\rho = 0.5$ ∘

Step 6: Calculating the correlation degree r_{ki} between the output of the k-th hidden layer's node (comparison sequence) and the reference sequence according to Eq. (10):

$$r_{ki} = r(x_k, x_i) = \frac{1}{n} \sum_{t=1}^{n} r(x_k(t), x_i(t)) \tag{10}$$

Taking $r_k = \max\limits_{i=1}^{m} \{r_{ki}\}$ as the degree of correlation between the k-th hidden layer's node and the expected output of the network.

Step 7: Repeating steps from 1 to 6 to find the correlation degree r_k between all hidden layer's nodes and the expected output;

Step 8: Sort the gray correlation degree. Sort the result in step 7 to get a gray correlation sequence. If the value of correlation degree between the output of a hidden layer's node and the expected output is less than the pre-set value, the corresponding hidden layer neurons can be deleted, and the network structure will be optimized.

Step 9: Repeat steps from 1 to 8 until the value is not less than the preset. The number of hidden layer's nodes is optimal, and the BP neural network structure is optimized.

The flow chart of the improved BP neural network algorithms based on GRA is shown in Figure 10.

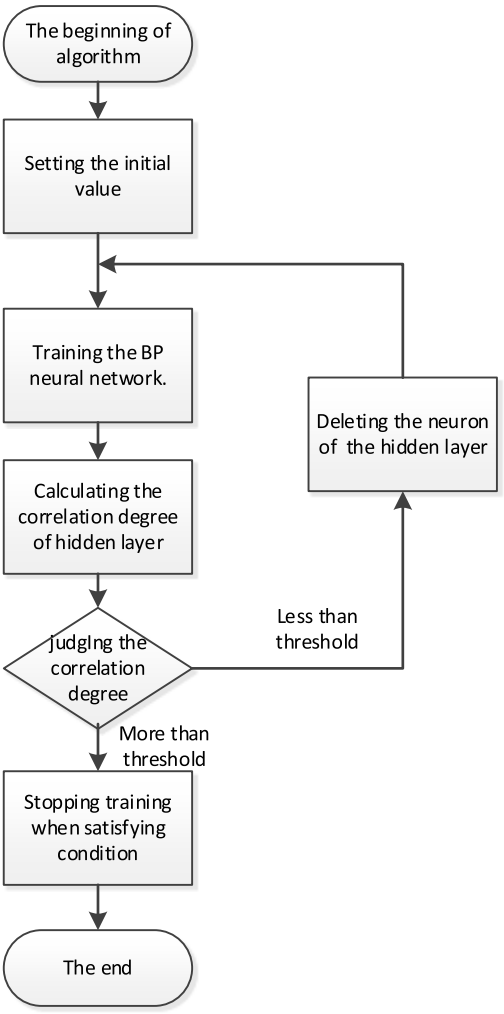

FIGURE 10. Flow chart of the improved BP neural network algorithm.

C. INITIAL SYSTEM PARAMETER SETTING

In the improved BP neural network fault diagnosis model, the structure of neural network was determined three layers according to the empirical formula, input nodes was set to 4, hidden layer tentative nodes was set to 12, output nodes was set to 5, the activation function of hidden layer chose logarithmic sigmoid function; the preset value of the correlation degree between the output of the hidden layer node and the expected output was set to $\varepsilon = 0.5$.The number groups of each fault samples was set to24. The input data needed to be normalized, and the number of hidden layer nodes was determined by Gray Relational Analysis.

The main training parameters of neural network algorithm were as follows:

.trainparam.max_fail = 5; % Max Confirmation Failures
.trainparam.goal = 0.001; % training target minimum error
.trainParam.epochs = 200; % training times
.trainParam.lr = 0.05; % learning rate
.trainParam.min_grad =1e-6; % minimum performance gradient

The rest of the parameters used the default values of Matlab.

In addition, the actual neural output of network should deviate from the ideal output, so we respectively set the threshold for the judgment fault diagnosis to 0.2 and 0.8.When the output is equal or greater than 0.8, it is determined that the actuator has a corresponding fault, when the output is equal or less than 0.2, it is determined that the actuator has no fault; when the output is between 0.2 and 0.8, it is determined that the fault diagnosis fails. Although it cannot determine what kind of fault had occurred, it still has reference significance.

V. ANALYSIS OF EXPERIMENT RESULTS

In order to verify the actual effect of the monitoring and diagnosis system which was designed in this paper, a experimental bench was built, as shown in Figure 11. It mainly included upper computer, DSP controller, current sensor, displacement sensor, ELA, drive circuit and other components.

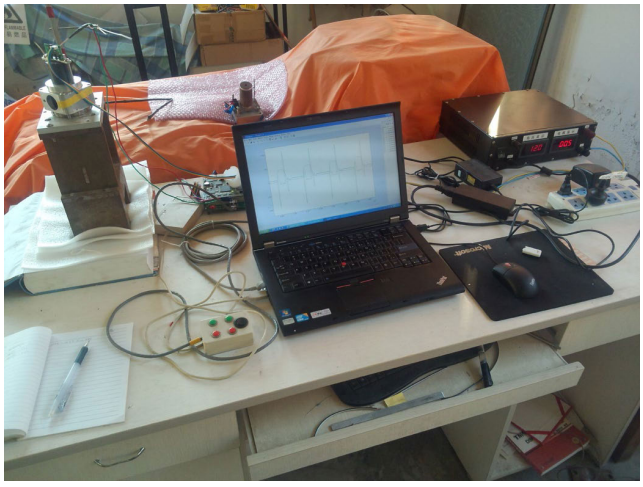

FIGURE 11. The monitoring and diagnosis experimental system of ELA under no-load situation.

A. RELIABILITY TEST OF ELECTROMAGNETIC LINEAR ACTUATOR

1) REPETITIVE EXPERIMENT

Electromagnetic linear actuator was easily affected by the external factors, so it was necessary to research the reliability

of the actuator. The experimental result of Electromagnetic linear actuator repeat test displacement curve was shown in the Fig12, and parameters of the experiment were as follows: setting the response time 3 ms, setting the maximal displacement 8 mm, setting cycle time 60 ms cycle, running 1000 times per minute, sampling 200 times. The experimental results validated that the actuator motion control had high precision, good repeatability, and the error in the allowed range.

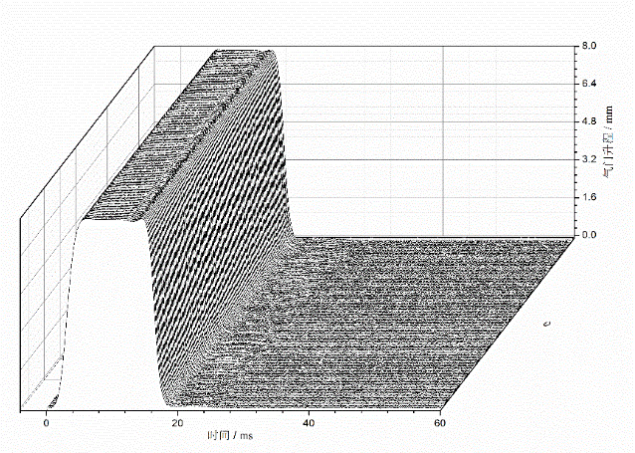

FIGURE 12. Repetitive experiment of electromagnetic linear actuator.

2) CONTINUOUS OPERATION RELIABILITY TEST

After continuously running 300 hours, the actuator was disassembled as shown in Figure 13, and the displacement error of the actuator was shown in Figure 14:

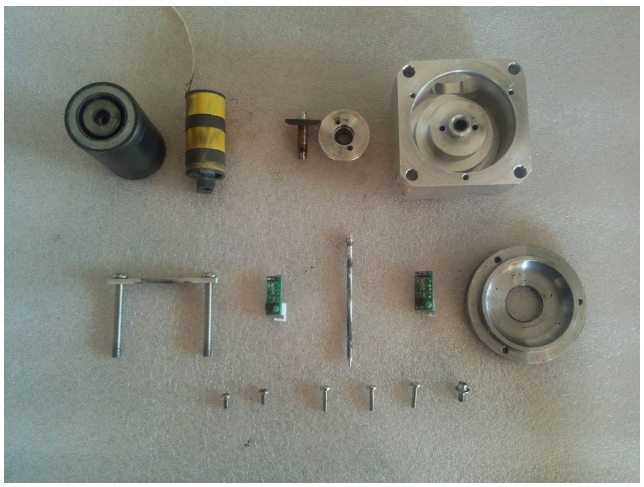

FIGURE 13. The disassembly picture of ELA after running 300 hours.

In the figure, the horizontal axis was time, and the vertical axis was the displacement error of the actuator. A set of data was taken every 12 hours, and there were 24 groups of data. The statistical data was drawn a line graph by Matlab. Judging from the figure, the actuator displacement offset was very small after running 300 hours, so the result verified that the performance of the actuator was excellent.

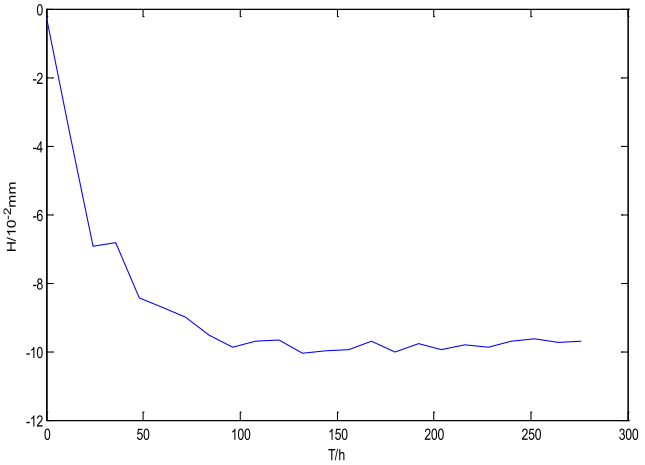

FIGURE 14. The displacement error of actuator during 300-hour running.

B. CHARACTERISTIC PARAMETER ANALYSIS OF ACTUATOR FAILURE

1) NORMAL OPERATION WITHOUT FAULT

Experimental current of electromagnetic linear actuator under normal operation were shown in FIG.15, and calculation results of the corresponding three characteristic parameters (mean value) were shown in Table 4.

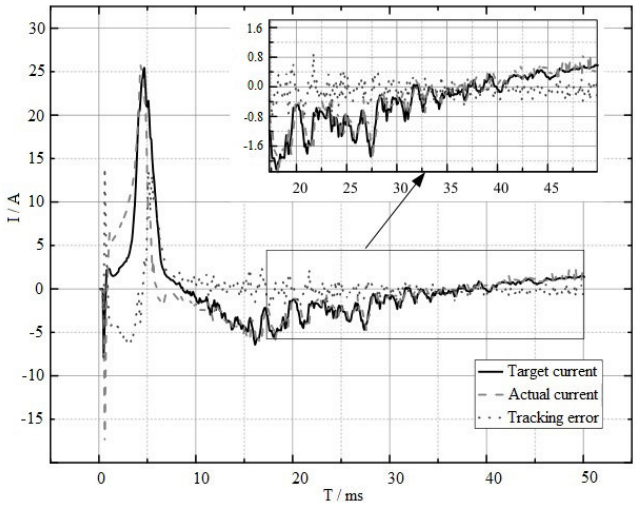

FIGURE 15. Experimental current of electromagnetic linear actuator under normal operation.

TABLE 4. The characteristic parameters of the actuator under normal operation.

Characteristic parameter	I_m (A)	K_i (A/ms)	I_a (A)
Normal operation	25.8	-24.4	0.57

2) SETTING THE FAULT AND IDENTIFYING THE CHARACTERISTIC PARAMETERS

When the ELA failed, some of its self-parameters were changed up to variations of the characteristic parameters. The faults were set during the experiment, and the test results were shown in Table 5, 6 and 7.

TABLE 5. The characteristic parameters variation of the actuator under short circuit state.

Characteristic parameter	I_m (A)	K_i (A/ms)	I_a (A)
Actuator short circuit	30.4	-33.6	30.4
Relative Variation Ratio	+20.4%	-37.7%	+5233%

TABLE 6. The characteristic parameters variation of the actuator under poor contact state.

Characteristic parameter	I_m (A)	K_i (A/ms)	I_a (A)
Poor contact	17.28	-10.83	0.56
Relative Variation Ratio	-33%	+50.6%	-1.75%

TABLE 7. The characteristic parameters variation of the actuator under mechanical fault state.

Characteristic parameter	I_m (A)	K_i (A/ms)	I_a (A)
Skeleton deformation	25.45	-23.8	0.85
Relative Variation Ratio	-1.36%	+2.46%	+49.1%

From the above data, it could be concluded that when the actuator had different faults, the apparent changes of the 3 characteristic parameters were compared with the normal operation in the range and the direction, so the result had high recognition degree. Therefore, it was verified that the method could achieve the purpose of fault diagnosis.

3) INTERFERENCE ANALYSIS

According to the analysis of the equation (1), it could be seen that the voltage disturbance and the load disturbance could affect the operating state of the actuator, and also change the characteristic parameter data of the real-time monitoring, which made the diagnosis of the neural network fault. Therefore, voltage disturbances and load disturbances needed to be analyzed separately. Now, 20% the voltage change and 10N load disturbance were respectively applied to the actuator, and the variation of the characteristic parameters analyzed was shown in Table 8 and 9.

TABLE 8. The characteristic parameters variation of the actuator under 20% voltage change.

Characteristic parameter	I_m (A)	K_i (A/ms)	I_a (A)
Voltage disturbance（20%）	31.1	29.23	0.685
Relative Variation Ratio	+20.6%	-19.8%	+20.1%

TABLE 9. The characteristic parameters variation of the actuator under10N load disturbance.

Characteristic parameter	I_m (A)	K_i (A/ms)	I_a (A)
load disturbance（10N）	25.6	23.76	1.385
Relative Variation Ratio	-0.78%	+0.26%	+143.1%

C. COMPARATIVE ANALYSIS OF FAULT DIAGNOSIS SYSTEMS BEFORE AND AFTER OPTIMIZATION

The experiment results contrasting pre-optimization and optimized BP neural network fault diagnosis system for each type of faults were shown in Table 10.

TABLE 10. Comparison of fault diagnosis results before and after optimization.

Fault State	Optimal state	sample size	Number of training	Number of hidden layer nodes	Number of optimizing	Number of right diagnosis	Fault recognition rate
Short circuit	Pre-	24	199	12	NULL	18	75%
	Post-	24	129	7	4	21	87.5%
Disconnection	Pre-	24	181	12	NULL	19	79.16%
	Post-	24	121	8	3	23	95.83%
Skeleton deformation	Pre-	24	161	12	NULL	20	83.33%
	Post-	24	112	7	4	22	91.67%
Disturbance	Pre-	24	158	12	NULL	19	79.17%
	Post-	24	91	8	4	22	91.67%

Through the above comparison results, the following conclusions could be drawn as follows:

(1) The accuracy of fault diagnosis of the optimized BP neural network algorithm based on GRA had a great improvement compared with the non-optimization method, and the average recognition accuracy reached 91.67%.

(2) The classification ability of the optimized BP neural network algorithm based on GRA was improved compared with the non-optimization method. Therefore, it was verified that the online fault diagnosis method of actuator proposed in this paper was feasible and reasonable. The operation state of actuator could be monitored real-time.

(3) The number of trainings of the optimized BP neural network algorithm based on GRA was significantly reduced compared with the non-optimization. It was indicated that this method improved the training speed, taking less time and having higher real-time performance.

D. MONITORING AND DIAGNOSIS DISPLAY OF THE OPERATION STATUS IN THE ENGINE VALVE-TRAIN

The on-line monitoring and diagnosis results of the operating state of the ELA realized by the upper computer software was shown in Figure 16. The monitoring and diagnosis results showed that in a certain cycle, the steady-state current values of the two actuators of No.1 EMVT were 24.6A and 24.5A. The valve opening stroke was 6mm and no fault occurred.

It could be proved that it was feasible to monitor the status, predict and diagnose the fault of the ELA by the

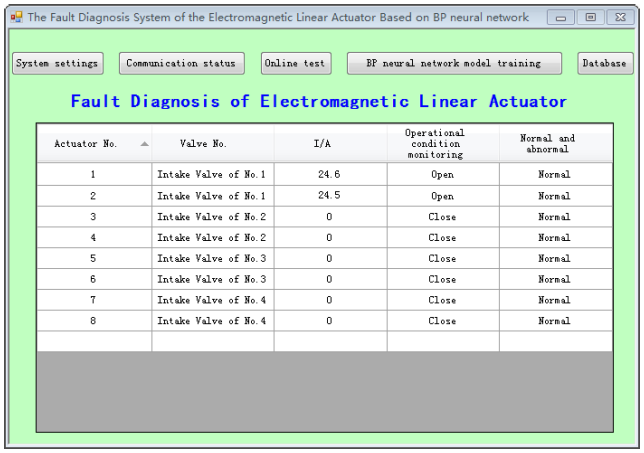

FIGURE 16. ELA and valve operating condition monitoring results.

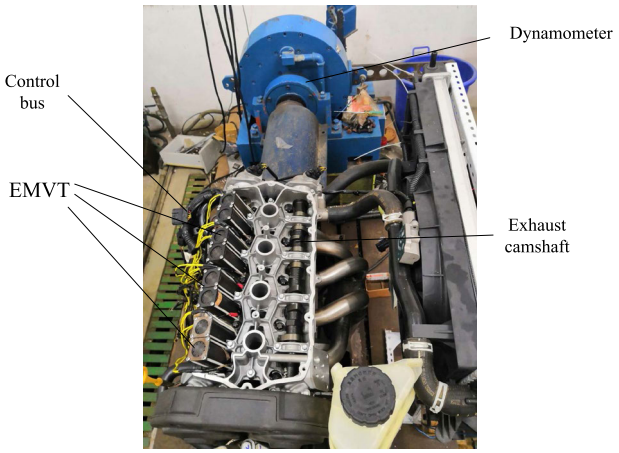

FIGURE 17. The new engine valve-train based on ELA(EMVT).

above method, and we applied it into the new engine valve-train, as shown in Fig17.

VI. SUMMARY

This paper mainly presented a real-time monitoring and fault diagnosis system of electromagnetic linear actuator based on machine learning method, which realized real-time monitoring health status, fault diagnosis and early warning during operation, and overcame many defects in the previous diagnosis methods. The system had the advantages of intelligence, informatization, low cost, real-time performance and reliability. The results showed that the fault diagnosis system had high accuracy, and the actuator fault could be pre-judged, analyzed and alerted early, which provided a powerful guarantee for the later application of the engine electromagnetic valve-train.

REFERENCES

[1] W. S. Chang, T. A. Parlikar, M. D. Seeman, D. J. Perreault, J. G. Kassakian, and T. A. Keim, "A new electromagnetic valve actuator," in *Proc. Power Electron. Transp.*, Oct. 2002, pp. 109–118.
[2] P. Mercorelli and N. Werner, "A hybrid actuator modelling and hysteresis effect identification in Camless internal combustion engines control," *Int. J. Model., Identificat. Control*, vol. 21, no. 3, pp. 253–263, 2014.
[3] Z. Dimitrova, M. Tari, P. Lanusse, F. Aioun, and X. Moreau "Robust control for an electromagnetic actuator for a Camless engine," *Mechatronics*, vol. 57, pp. 109–128, Feb. 2019.
[4] L. Liu and S. Chang, "Motion control of an electromagnetic valve actuator based on the inverse system method," *Proc. Inst. Mech. Eng. D, J. Automobile Eng.*, vol. 226, no. 1, pp. 85–93, Jan. 2012.
[5] L. Liu and S. Chang, "A moving coil electromagnetic valve actuator for camless engines," in *Proc. Int. Conf. Mechatron. Automat.*, Aug. 2009, pp. 176–180.
[6] M. Nakamura, S. Hara, and Y. Yamada, "A continuous variable valve event and lift control device (VEL) for automotive engines," SAE Tech. Paper 2001-01-0244, 2001, pp. 126–136.
[7] P. Mercorelli, K. Lehmann, and S. Liu, "Robust flatness based control of an electromagnetic linear actuator using adaptive PID controllerm," in *Proc. IEEE Conf. Decis. Control*, Dec. 2003, pp. 3790–3795.
[8] S. Braune, S. Liu, and P. Mercorelli, "Design and control of an electromagnetic valve actuator," in *Proc. IEEE Int. Conf. Control Appl.*, Oct. 2006, pp. 1657–1662.
[9] J. Lu and S. Chang, "Precise motion control of an electromagnetic valve actuator with adaptive robust compensation of combustion force," *J. Franklin Inst.*, vol. 356, no. 4, pp. 1750–1770, Mar. 2019.
[10] J. Lu and S. Chang, "A trajectory planning-based energy-optimal method for an EMVT system," *CMES-Comput. Model. Eng. Sci.*, vol. 118, no. 1, pp. 91–109, Oct. 2019.
[11] J. Lu, S. Chang, L. Liu, and X. Fan, "Point-to-point motions control of an electromagnetic direct-drive gas valve," *J. Mech. Sci. Technol.*, vol. 32, no. 1, pp. 363–371, Jun. 2018.
[12] P. Mercorelli, "An adaptive and optimized switching observer for sensorless control of an electromagnetic valve actuator in camless internal combustion engines," *Asian J. Control*, vol. 16, no. 4, pp. 959–973, Jul. 2014.
[13] M. Manana, A. Arroyo, A. Ortiz, C. J. Renedo, S. Perez, and F. Delgado, "Field winding fault diagnosis in DC motors during manufacturing using thermal monitoring," *Appl. Thermal Eng.*, vol. 31, no. 5, pp. 978–983, 2011.
[14] A. Glowacz, "Diagnostics of DC and induction motors based on the analysis of acoustic signal," *Meas. Sci. Rev.*, vol. 14, no. 5, pp. 257–262, Oct. 2014.
[15] P. S. Bhowmik, S. Pradhan, and M. Prakash, "Fault diagnostic and monitoring methods of induction motor: A review," *Int. J. Appl. Control, Elect. Electron. Eng.*, vol. 1, no. 1, pp. 1–18, 2013.
[16] L. Hou and N. W. Bergmann, "Novel industrial wireless sensor networks for machine condition monitoring and fault diagnosis," *IEEE Trans. Instrum. Meas.*, vol. 61, no. 10, pp. 2787–2798, Oct. 2012.
[17] L. H. Wang, X. P. Zhao, J. X. Wu, Y. X. Xie, and Y. H. Zhang, "Motor fault diagnosis based on short-time Fourier transform and convolutional neural network," *Chin. J. Mech. Eng.*, vol. 30, no. 6, pp. 1357–1368, 2017.
[18] L. Hou and N. W. Bergmann, "Induction motor fault diagnosis using industrial wireless sensor networks and Dempster-Shafer classifier fusion," in *Proc. 37th Annu. Conf. IEEE Ind. Electron. Soc.*, Nov. 2011, pp. 2992–2997.
[19] X. Wang, X. B. Xu, and Y. D. Ji, "Fault diagnosis using neuro-fuzzy network and Dempster-Shafer theory," in *Proc. Int. Conf. Wavelet Anal. Pattern Recognit.*, Jul. 2012, pp. 137–147.
[20] A. Jawadekar, S. Paraskar, S. Jadhav, and G. Dhole, "Artificial neural network-based induction motor fault classifier using continuous wavelet transform," *Syst. Sci. Control Eng. Open Access J.*, vol. 2, no. 1, pp. 684–690, Dec. 2014.
[21] W. Glowacz and Z. Glowacz, "Diagnostics of separately excited DC motor based on analysis and recognition of signals using FFT and Bayes classifier," *Arch. Elect. Eng.*, vol. 64, no. 1, pp. 29–35, Mar. 2015.
[22] A. Glowacz, "DC motor fault analysis with the use of acoustic signals, Coiflet wavelet transform, and K-nearest neighbor classifie," *Arch. Acoust.*, vol. 40, no. 3, pp. 321–327, Sep. 2015.
[23] K. H. Kim, "Simple online fault detecting scheme for short-circuited turn in a PMSM through current harmonic monitoring," *IEEE Trans. Ind. Electron.*, vol. 58, no. 6, pp. 2565–2568, Jun. 2010.
[24] N. Mehala, "Condition monitoring and fault diagnosis of induction motor using motor current signature analysis," M.S. Thesis, Dept. Elect. Eng., Nat. Inst. Technol., Kurushetra, India, 2010.
[25] M. Aktas and V. Turkmenoglu, "Wavelet-based switching faults detection in direct torque control induction motor drives," *IET Sci., Meas. Technol.*, vol. 4, no. 6, pp. 303–310, Nov. 2010.

[26] M. Iorgulescu, R. Beloiu, and M. O. Popescu, "Vibration monitoring for diagnosis of electrical equipment's faults," in *Proc. 12th Int. Conf. Optim. Elect. Electron. Equip.*, May 2010, pp. 493–499.
[27] R. Yan, R. X. Gao, and X. Chen, "Wavelets for fault diagnosis of rotary machines: A review with applications," *Signal Process.*, vol. 96, pp. 1–15, Mar. 2014.
[28] J. Seshadrinath, B. Singh, and B. K. Panigrahi, "Incipient turn fault detection and condition monitoring of induction machine using analytical wavelet transform," *IEEE Trans. Ind. Appl.*, vol. 50, no. 3, pp. 2235–2242, May/Jun. 2013.
[29] Y. Da, X. Shi, and M. Krishnamurthy, "Health monitoring, fault diagnosis and failure prognosis techniques for brushless permanent magnet machines," in *Proc. IEEE Vehicle Power Propuls. Conf.*, Sep. 2011, pp. 1–7.
[30] S. H. Kia, H. Henao, and G. A. Capolino, "Efficient digital signal processing techniques for induction machines fault diagnosis," in *Proc. IEEE Workshop Elect. Mach. Design, Control Diagnosis (WEMDCD)*, Mar. 2013, pp. 232–246.
[31] J. Dai, S. Chang, and L. Liu, "Optimization analysis of electromagnetic linear actuator's radial array permanent magnets," *Int. J. Appl. Electromagn. Mech.*, vol. 47, no. 2, pp. 441–451, Jan. 2015.
[32] W. Jin, Z. J. Li, and L. S. Wei, "The improvements of BP neural network learning algorithm," in *Proc. 5th Int. Conf. Signal Process.*, vol. 3, Aug. 2000, pp. 1647–1649.
[33] L. Feng, "Research on the identification coefficient of relational grade for grey system," *Syst. Eng. Theory Pract.*, vol. 6, 1997.
[34] Y. Dong and Z. Duan, "A new determination method for identification coefficient of grey relational grade," *J. Xi'an Univ. Archit. Technol.*, vol. 4, no. 40, pp. 589–592, 2008.
[35] G. Ma and Y. Bai, "The research and application on building a forecasting model with grey theory and neural network," *Microelectron. Comput.*, vol. 25, no. 1, pp. 153–155, 2008.
[36] B. Su, L. Liu, and F. Yang, "Research of artificial neural network forecasting model based on grey relational analysis," *Syst. Eng.-Theory Pract.*, vol. 9, pp. 98–104, Sep. 2008.
[37] D. Niu and J. Lu, "Gray neural network forecast of power loads based on relaitonal analysis method," *East China Electr. Power*, vol. 35, no. 8, pp. 60–62, 2007.
[38] S. Qian, S. Zhou, and W. Chang, "A diagnosis method for diesel engine wear fault based on grey rough set and SOM neural network," in *Safety and Reliability–Safe Societies in a Changing World*. Boca Raton, FL, USA: CRC Press, 2018, pp. 995–1002.

TONGJUN GUO was born in Jingdezhen, Jiangxi, China, in 1985. He is currently pursuing the Ph.D. degree with the Nanjing University of Science and Technology, Jiangsu, China. He had participated in the projects of the National Natural Science Foundation of China and the Natural Science Foundation of Jiangsu Province. He has published several research papers in the relevant research fields. His research interests include motion control and state monitoring of high performance electromagnetic linear actuator.

SIQIN CHANG received the Ph.D. degree from the Huazhong University of Science and Technology, Wuhan, China, where he is currently a Professor and a Doctoral Supervisor. He has authored two books, more than 150 articles, and more than 10 inventions. He has published many research papers in scholarly journals in his research areas. His research interests include the design, simulation, and optimization of vehicle power plant, and the applications of high-performance electromagnetic linear actuator. He is also a member of the National 863 Plan Expert Library.

ZHIQIANG CHEN was born in Yancheng, China, in 1995. He is currently pursuing the master's degree with the Nanjing University of Science and Technology. During the study period, he was supported by the National Natural Science Foundation Fund and the Shanghai Aerospace Science and Technology Innovation Fund. He has published research papers in related fields. His research interest includes the vehicle braking-by-wire system research.

HANGANG HUANG was born in Jingdezhen, China, in 1985. He is currently pursuing the master's degree. He is currently an English Teacher with the College of Technology and Art Jingdezhen Ceramic Institute. He has published several research papers in relevant research fields. During 15 years of teaching, he has won several prizes and certificates in different contests and several titles of honor such as Outstanding Teacher, Teaching Expert, and Advanced Persons in Teaching.

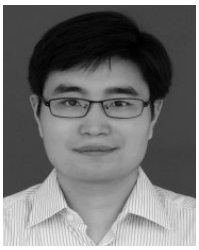

JIANGTAO XU was born in Gaoyi Town, China, in 1982. He received the B.S. degree in marine engineering from Guangdong Ocean University, China, in 2002, the M.Sc. and Ph.D. degrees in marine engineering from the Jiangsu University of Science and Technology, China, in 2009, and the Ph.D. degree in mechanical engineering from the Nanjing University of Science and Technology, China, in 2018.

He is currently an Associate Professor in machine design with the Mechanical Engineering Department, Nanjing Institute of Technology, Nanjing, China. His research interests include performance optimization and simulation of power machinery, durability analysis, and the experiment of mechanical mechanism. His awards and honors include the Young Teacher of the Project Blue in Jiangsu Province, China.